Modeling the Solvent Effect on the Tacticity in the Free Radical Polymerization of Methyl Methacrylate

ARTICLE *in* MACROMOLECULES · JUNE 2010

Impact Factor: 5.8 · DOI: 10.1021/ma100608g

7 AUTHORS, INCLUDING:

Isa Değirmenci
Ondokuz Mayıs Üniversitesi
12 PUBLICATIONS **191** CITATIONS
SEE PROFILE

Viktorya Aviyente
Bogazici University
146 PUBLICATIONS **1,447** CITATIONS
SEE PROFILE

Karen Hemelsoet
Ghent University
56 PUBLICATIONS **872** CITATIONS
SEE PROFILE

Michel Waroquier
Ghent University
417 PUBLICATIONS **8,264** CITATIONS
SEE PROFILE

DOI: 10.1021/ma100608g

Macromolecules
ARTICLE

Modeling the Solvent Effect on the Tacticity in the Free Radical Polymerization of Methyl Methacrylate

İsa Değirmenci, Şükrü Eren, and Viktorya Aviyente*

Chemistry Department, Boğazici University, 34342, Bebek, Istanbul, Turkey

Bart De Sterck, Karen Hemelsoet, Veronique Van Speybroeck, and Michel Waroquier

Center for Molecular Modeling, Ghent University, Technologiepark 903, 9052 Zwijnaarde, Belgium, and QCMM-Alliance Ghent-Brussels, Belgium

Received March 21, 2010; Revised Manuscript Received May 15, 2010

ABSTRACT: The control of stereochemistry in the free radical polymerization of methyl methacrylate (MMA) is important because the physical properties of PMMA are often significantly affected by the main-chain tacticity. In this study, the role of the solvent on the tacticity of MMA polymerization has been investigated by considering the propagation rate constants for the syndiotactic and isotactic free radical polymerization of MMA in vacuum, in methanol (CH_3OH), and in 1,1,1,3,3,3-hexafluoro-2-(trifluoromethyl)propan-2-ol ($(CF_3)_3COH$). All geometry optimizations have been carried out with the B3LYP/6-31+G(d) methodology. The kinetics of the propagating dimer have been evaluated with the B3LYP/6-31+G(d), B3LYP/6-311+G(3df,2p), MPWB1K/6-311+G(3df,2p), and B2PLYP/6-31+G(d) methodologies. The role of the solvent has been investigated by using explicit solvent molecules and also by introducing a polarizable continuum model (IEF-PCM) with a dielectric constant specific to the solvent. Experimentally, the free radical polymerization of MMA in $(CF_3)_3COH$ is found to be highly syndiotactic (*rr* = 75% at 20 °C): the stereoeffects of fluoroalcohols are claimed to be due to the hydrogen-bonding interaction of the alcohols with the monomers and growing species. This modeling study has revealed the fact that the solvents CH_3OH and $(CF_3)_3COH$, which are H-bonded with the carbonyl oxygens located on the same side of the backbone hinder the formation of the isotactic PMMA to some extent. Methanol is less effective in reducing the isotacticity because of its small size and also because of the relatively loose hydrogen bonds (∼1.9 Å) with the carbonyl oxygens. The methodologies used in this study reproduce the solvent effect on the free radical polymerization kinetics of MMA in a satisfactory way.

Introduction

The mechanical, thermal, and chemical properties of polymers substantially depend on their primary structures as represented by tacticities, molecular weights, and their distributions.[1] The control of tacticity and molecular weight for synthetic polymers contributes to the development of new materials.[2] The precise control of the molecular weight and/or the chain microstructure during radical polymerization is one of the important issues in the field of polymer synthesis because the polymer properties, such as toughness, solvent resistance, surface properties, and thermal resistance, are significantly influenced by their stereoregularity.[3] The stereoregularity of a polymer main chain is referred to as tacticity. Tacticity deals with the relationship between two adjacent monomer units consisting of meso (*m*) and racemo (*r*) diads. In general, stereocontrol based on radical polymerization is difficult to attain because of the planar characteristics of the propagating radical at the chain-end carbon.[4] Although most of the stereospecific polymerizations were reported for the coordination polymerizations of olefins such as propylene, the stereocontrol during free radical polymerization reactions has recently become possible.[5] Many attempts to produce stereospecific or stereoregular polymers have been made in confined media, such as the solid state, inclusion compounds, porous materials, and templates.[6,7] In solution polymerization, it is more difficult to provide a stereospecific environment around the growing radical center because the monomer and growing radical species move freely and diffuse in the reaction media. Therefore, vinyl monomers ordinarily produce polymers with an inherent tacticity specific to their chemical structures. From the viewpoint of production cost, solvent or additive-mediated systems might be the most promising solutions to obtain stereospecific polymers.

Okamoto and co-workers have reported the synthesis of highly stereocontrolled polymethacrylates,[8] polyacrylamides,[9−11] and polymethacrylamides[10−12] through radical polymerization using Lewis acids such as rare earth metal trifluoromethanesulfonates. Furthermore, fluorinated alcohols play an efficient role in controlling the stereospecificity of radical polymerizations of vinyl monomers.[13−15] A relevant study on how tacticity can arise by chain-end control in free radical polymerization of acrylates is given by Tanaka and Niwa.[16] The study suggested that the growing polymer radical end could control the stereochemistry of free radical polymerization depending on the *s-trans* and *s-cis* conformations of the monomer. Many industrially important vinyl polymers including PMMA are produced by free radical polymerization, which is generally poor in stereocontrol. Hence, the development of stereoregulation methods for radical polymerization can contribute to the industrial production of polymers with improved properties.[17] The control of the stereochemistry in MMA polymerization is important because the physical properties of PMMA are often significantly affected by the main-chain tacticity. In the free radical polymerization of MMA three different products are to be expected: syndiotactic (*rr*), isotactic (*mm*), and heterotactic (*mr*). Isobe et al.

*To whom correspondence should be addressed.

 Published on Web 06/08/2010

Table 1. Tacticity in the Free Radical Polymerization of MMA in Various Solvents at 20 °C[13c]

	solvent	tacticity *mm*/*mr*/*rr*
1	bulk	3/31/66
2	CH_3OH	3/32/66
3	$(CF_3)_3COH$	1/24/75

have enhanced the syndiotactic specificity of PMMA by using fluoroalcohols: the polymerization of MMA in perfluoro-*tert*-butyl alcohol (PFTB) $(CF_3)_3COH$ at −98 °C was achieved with the highest syndiotacticity (*rr* = 93%), whereas the syndiotacticity of PMMA is only 85% in methanol at −78 °C. Table 1 displays the tacticity ratios in the free radical polymerization of MMA at 20 °C.

Another issue concerns the solvent influence on the propagation kinetics in free radical polymerization. For a long time it was assumed that the solvent effects on the rate coefficients were rather small.[18] Propagation rate coefficients for styrene and methyl methacrylate (MMA) polymerizations in a wide variety of solvents (acetonitrile, dimethylformamide, anisole, methyl isobutyrate, bromobenzene, benzene, and 1,2-dichloroethane) only change mostly by around 10% (see review of S. Beuermann and references cited therein[18]). On the other hand, certain solvents, such as benzyl alcohol,[19,20] dimethylsulfoxide,[20] *N*-methylpyrrolidinone,[20] 2,6-dithiaheptane,[21] and 1,5-dithiacyclooctane,[21] turn out to induce a significant increase of k_p. In many cases hydrogen bonding is responsible for this observed increase. Experiments provided by data for acrylamide and *N*-isopropylacrylamide (NIPAM) suggest a strong increase of k_p upon addition of water to the system.[22]

In this study, the role of methanol (CH_3OH) and 1,1,1,3,3,3-hexafluoro-2-(trifluoromethyl)propan-2-ol ($(CF_3)_3COH$) on the tacticity of MMA polymerization will be considered by examining the propagation rate constants for the syndiotactic and isotactic free radical polymerization of MMA.

Computational Procedure

The B3LYP method combined with 6-31+G(d) basis set within the Gaussian 03 program package[23] was chosen as a cost-effective and accurate method for geometry optimizations.[24] To verify that the transition states indeed connect the products and prereactive complexes, intrinsic reaction coordinate (IRC)[25] calculations were performed. All transition states are characterized by only one imaginary frequency and are true first-order saddle points on the potential energy surface.

The energetics and kinetics have been evaluated with the MPWB1K/6-311+G(3df,2p)//B3LYP/6-31+G(d), B3LYP/6-311+G(3df,2p)//B3LYP/6-31+G(d), B3LYP/6-31+G(d)//B3LYP/6-31+G(d), and B2-PLYP/6-31+G(d)//B3LYP/6-31+G(d) methodologies.

The MPWB1K method has proven to be very successful for describing thermochemistry, reaction kinetics, hydrogen bonding, and weak interactions.[26−29] The B2-PLYP method, which combines the BLYP[30] functional with Hartree−Fock exchange and a perturbative second-order correlation part, is also used since it is a promising functional with a high accuracy, taking into account dispersion interactions.[31]

To study the solvent effect, we first apply an explicit solvent model. Isobe et al. have shown experimentally that the concentration of the MMA−$(CF_3)_3COH$ complex was highest when the molar ratio of the two components was approximately 1/1, indicating that the stoichiometry of the reaction was 1/1.[13c] The interaction of the MMA monomer (M) and the radical ($R^\bullet$) with the solvent (S) has been considered as a two-step mechanism that involves a fast preequilibrium between the reactants and the solvent (M···S and S···$R^\bullet$) followed by the formation of a prereactive complex (S−R−M−S)$^\bullet$; this procedure was performed earlier in ref 32.

Scheme 1. Representation of the Role of the Prereactive Complex in the Apparent Rate Coefficient

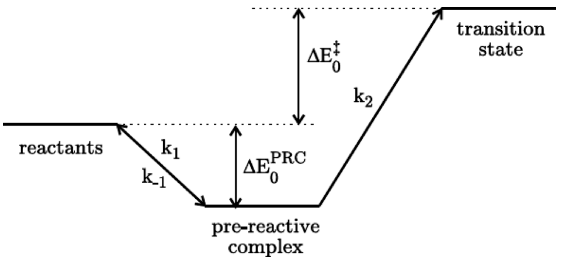

Step 1:

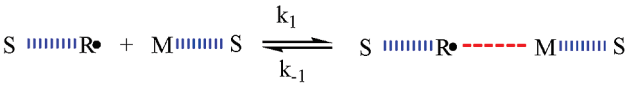

Step 2:

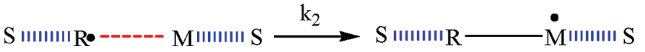

If k_1 and k_{-1} are the rate constants for the forward and reverse reactions in the first step and k_2 corresponds to the second step, the apparent kinetic parameters can be split up in two contributions: the rate coefficient (k_2) and the equilibrium constant K_1 for the formation of the prereactive complex (PRC).[33] A schematic representation of the role of the prereactive complex in the apparent reaction rate coefficient is given in Scheme 1.

$$k_{app} = K_1 k_2 = \frac{k_2 k_2}{k_{-1} + k_2} \approx \frac{k_1 k_2}{k_{-1}} \quad (1)$$

with the equilibrium constant of the fast equilibrium between the reactants and the prereactive complex obeying the basic statistical thermodynamic principles

$$K_1 = \frac{Q_{PRC}}{Q_R} \exp[\Delta E_0^{PRC}/RT] \quad (2)$$

ΔE_0^{PRC} represents the molar energy difference at 0 K between the reactants and the PRC including zero-point vibration energies (ZPVE) .

Q_{PRC} and Q_R are the prereactive complex and the reactants partition functions, respectively.

Similarly, the classical TST formula can be used to calculate k_2[34]

$$k_2 = \sigma \frac{k_B T}{h} \frac{Q_{TS}}{Q_{PRC}} \exp[-(\Delta E_0^{\ddagger} + \Delta E_0^{PRC})/RT] \quad (3)$$

with $\Delta E_0^{\ddagger}$ the reaction barrier for the transition state including ZPVE. σ is the reaction path degeneracy that accounts for the number of equivalent reaction paths. k_B represents Boltzmann's constant, T is the temperature, and h is Planck's constant. Finally, the apparent reaction rate coefficient k_{app} becomes

$$k_{app} = \sigma \frac{k_B T}{h} \frac{Q_{TS}}{Q_R} \exp[-\Delta E_0^{\ddagger}/RT] \quad (4)$$

This also means that calculating the reaction rate from separated reactants will result in exactly the same rate coefficients as compared to calculating the product of the equilibrium constant K_1 and the unimolecular reaction rate k_2. Although one could start from the separated reactants, the PRC concept is very valuable to get more insight into the role of the solvent molecules and their ability to stabilize the transition state.[32]

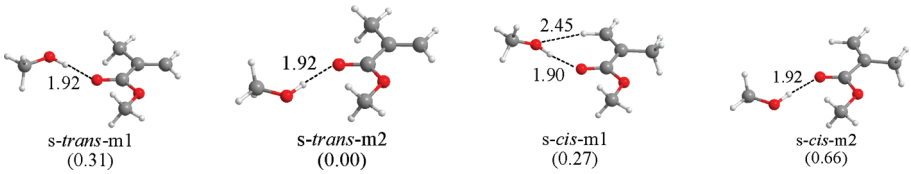

Figure 1. Relative energies (kcal/mol) of the *s-cis* and *s-trans* conformers of MMA with CH_3OH (MPWB1K/6-311+G(3df,2p)//B3LYP/6-31+G(d)).

Scheme 2. Representation of Isotactic and Syndiotactic Radical Polymerization of MMA

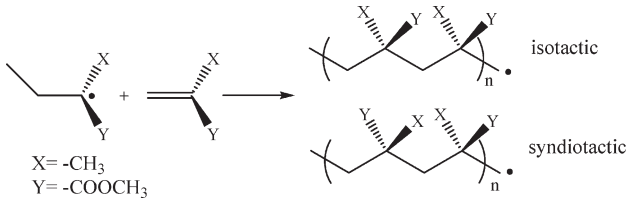

Equation 4 can be rewritten in terms of the molecular Gibbs free energy difference $\Delta G^{\ddagger}$ between the activated complex and the reactants (with inclusion of zero point vibration energies):

$$k_{app} = \kappa \frac{k_B T}{h} \frac{RT}{p^{\theta}} \exp[-\Delta G^{\ddagger}/RT] \quad (5)$$

where R represents the universal gas constant and κ the transmission coefficient which is assumed to be about 1 and p^{θ} is the standard pressure 10^5 Pa (1 bar).[35]

In the case where the solvent effect is considered implicitly as a polarized continuum medium, the effect of the environment was taken into account by use of the self-consistent reaction field (SCRF) theory, utilizing the integral equation formalism−polarizable continuum (IEF-PCM) model.[36] In the case where the solvent effect has been modeled explicitly and implicitly the effect of the solvent is modeled as the sum of two contributions: one resulting from the explicit coordination with the individual solvent molecules in the reactants and transition states and one originating from the bulk solvent effect as in earlier publications.[37]

Results

The free radical polymerization of MMA is known to start by the generation of free radicals from the nonradical species (initiator).

$$I \xrightarrow{k_d} R^{\bullet} \quad \text{(initiation)}$$

The radical $R^{\bullet}$, taken in this study as the methyl ($CH_3^{\bullet}$) radical, adds to the acrylate monomer and forms a backbone with three C atoms. This radical species then adds to the monomer to generate the propagating polymer chain (propagation reaction). $CH_3^{\bullet}$ addition to the carbon−carbon double bond (C=C) was investigated elaborately by Radom et al.[38] Radical addition reaction kinetics of some vinyl monomers was modeled by Coote et al.[39−41] Head-to-tail propagation was assumed to be the most favorable mode of attack.[34,42] Several groups have modeled the structure−reactivity relationship of various acrylates and methacrylates by using quantum chemical tools.[27−29,41,43]

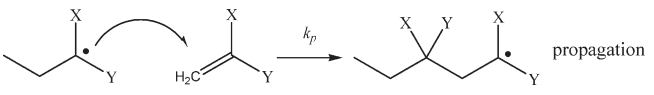

This study aims in elucidating the origins of the syndiotactic/isotactic stereospecificity in the free radical polymerization of MMA, as depicted in Scheme 2.

Scheme 3. Most Stable Conformations of MMA[a]

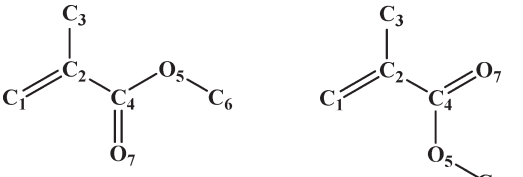

s-*cis* $C_1C_2C_4O_7 = 0°$ (0.39)

s-*trans* $C_1C_2C_4O_7 = 180°$ (0.00)

[a] Relative energies in (kcal/mol) are given in parentheses (MPWB1K/6-311+G(3df,2p)//B3LYP/6-31+G(d)).

Scheme 4. Most Stable Conformations of MMAR[a]

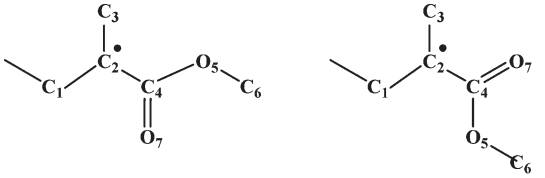

syn-r $C_1C_2C_4O_7 = 0°$ (0.00)

anti-r $C_1C_2C_4O_7 = 180°$ (0.01)

[a] Relative energies in (kcal/mol) are given in parentheses (MPWB1K/6-311+G(3df,2p)//B3LYP/6-31+G(d)).

A. Free Radical Polymerization of MMA in CH_3OH as Solvent. *MMA−CH_3OH Complex*. In vacuum, the most stable conformation of MMA is found to be *s-trans* ($C_1C_2C_4O_7 = 180°$) as shown in Scheme 3. A conformational search for the MMA−CH_3OH complex was carried out in order to find out the most stable solvated structures of the monomer−solvent entity. For both *s-cis* and *s-trans* conformations the carbonyl oxygen is the only site to be prone to hydrogen bonding. Among the conformations shown in Figure 1, complexation to the *s-trans* conformation of MMA from its methoxy side renders this complex (*s-trans*-m2) slightly more stable than the others. The relative energies of the *s-cis*/*s-trans* monomer−CH_3OH complexes range from 0.3 to 0.7 kcal/mol (Figure 1).

MMAR−CH_3OH Complex. In the gas phase the *syn* and *anti* conformation of the radical are almost isoenergetic, and both have been considered for the formation of possible MMAR−CH_3OH complexes (Scheme 4). Complexation of the radical with the methanol solvent does not alter significantly the energetics: the difference in binding energy between the *syn*-r and *anti*-r remains negligible (Figure 2). CH_3OH preferentially binds to the carbonyl oxygen (*syn*-r1 and *syn*-r2) of the radical. The global minimum for the *syn* conformer of the radical is found to be the structure where methanol forms a hydrogen bond with the carbonyl oxygen with the methyl group away from the propagating chain; the *anti* conformation is slightly more stable than *syn* conformation. The relative energies of the radicals range from 0.1 to 0.5 kcal/mol (Figure 2).

Transition Structures and Prereactive Complexes. The radical can attack the double bond of the monomer to yield

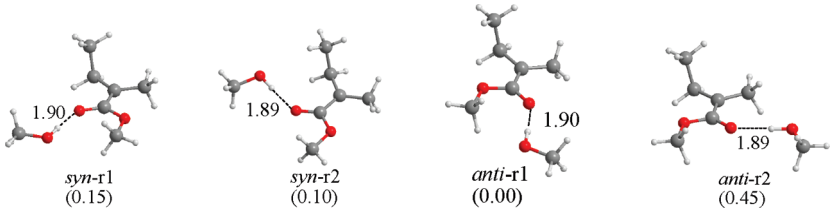

Figure 2. Relative energies (kcal/mol) of the various conformations of the MMAR−CH_3OH complexes (MPWB1K/6-311+G(3df,2p)//B3LYP/6-31+G(d).

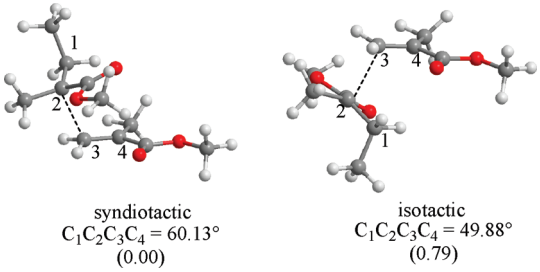

Figure 3. Dimeric transition structures for the free radical polymerization of MMA in vacuo (MPWB1K/6-311+G(3df,2p)//B3LYP/6-31+G(d)).

Scheme 5. Stereoselective Radical (*syn*) Addition to MMA (*s-cis* and s-*trans*)

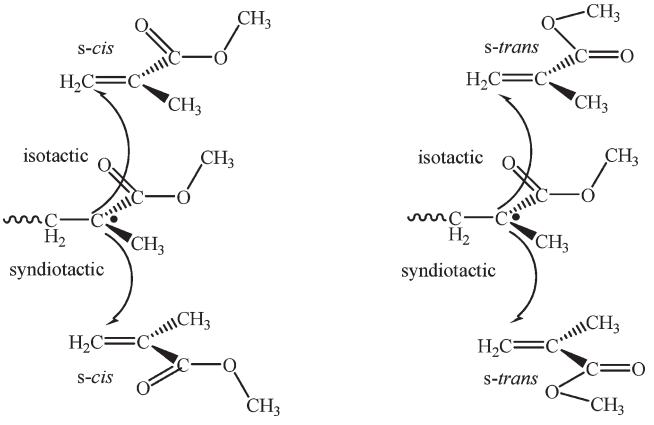

either the isotactic or syndiotactic dimer based on the relative orientation of the two species (Scheme 5). As already discussed in a previous study of the authors, the attack of the radical to the monomer is gauche in the syndiotactic and isotactic polymer chains.[43a]

Solvation of the transition state is studied by including only one methanol solvent molecule per unit. In this picture the propagating radical attacks the monomer while a solvent molecule −CH_3OH− can form a hydrogen bond with the monomer (MMA) and the propagating radical (MMAR) as depicted in Scheme 6. Our previous study[43a] has shown that the most stable transition structures correspond to the attack of the monomeric radical of MMA in a *syn* conformation to the *s-cis* isomer of the monomer. The solvent can approach the monomer and the radical either from the direction in between the propagating species (inner approach -i) or from outside (outer approach -o). As displayed in Scheme 6, alternative approaches of the solvent molecule to the propagating syndiotactic and isotactic polymer chains have been modeled; the most stable ones in each case have been reported. The nomenclature *syn*-oo, *syn*-oi, *syn*-io, *syn*-ii has been used to identify the approach of the solvent to the syndiotactic chain; similar notation *iso*-oo, *iso*-oi, *iso*-io, *iso*-ii has been employed for the isotactic chain.

In the transition structures for the syndiotactic and isotactic propagating chains the carbonyl oxygen coordinates with methanol with distances varying from 1.86 to 1.91 Å, while the oxygen atom of the methanol is also involved in secondary long-range stabilizing interactions with the methyl hydrogens in close proximity (2.43−2.52 Å). The presence of these bridge-type hydrogen bonds are decisive for determining the most stable transition structures. They elucidate mainly why syndiotactic structures are slightly better stabilized by the solvent by 1−3 kcal/mol (MPWB1K/6-311+G(3df,2p)//B3LYP/6-31+G-(d), Figure 4). In all transition structures the forming C---C bond distances between the monomer and the radical vary between 2.24 and 2.26 Å. Also note that even though the nomenclature i(inner)/o(outer) is adopted for the approach of methanol to the dimeric chain, optimizations have led to structures where the methanol molecules H-bonded to the carbonyl oxygens lie more or less between the monomer and radical moieties in the dimeric structures.

IRC calculations have yielded the prereactive complexes corresponding to the transition structures. The prereactive complexes correspond to stationary points along the potential energy surface of the propagation reaction where the two CH_3OH solvent molecules keep the monomer and the propagating radical in close proximity to each other before these two species have the proper orientation to react. The most favorable reaction paths for both syndiotactic and isotactic dimerizations are shown in Figures 5 and 6. The syndiotactic polymer chain is better stabilized and reacts faster than the isotactic polymer chain ($\Delta E_0^{\ddagger}$ amounts to 3.95 and 5.40 kcal/mol, respectively).

The kinetics of all the paths corresponding to the transition structures depicted in Figure 4 have been considered; the contribution of the *syn*-ii and *iso*-oo structures is found to be higher than the others. As shown in Figure 5, Figure 6, and Table 2 the energy barrier for the syndiotactic reaction (*syn*-ii) is smaller than the one for the isotactic reaction (*iso*-oo) about 1.45 kcal/mol by using explicit solvent. This difference is mainly due to the presence of steric effects in the isotactic transition structure. However, as displayed in Table 3, the ratio k_{syn}/k_{iso} is smaller than the one that would be expected based on energy barriers; this is due to entropic contributions to the rate constants. The vibrational partition function of the isotactic dimeric transition structure (0.74×10^{31}) is greater than the one of the syndiotactic structure (0.17×10^{30}) as a result of greater disorder in the former. The isotactic structure is more disordered due to the presence of the pendant groups on the same side of the backbone. Overall, the isotactic structure is favored entropically ($\Delta G^{\ddagger}$), whereas the syndiotactic structure is favored energetically ($\Delta E_0^{\ddagger}$), as shown in Table 2. The reaction is exothermic slightly in favor of the syndiotactic path. In Table 3 the reaction channels have been considered as concurrent reactions where the sum of the reaction rate constants for the syndiotactic (k_{syn}) and isotactic (k_{iso}) paths have been evaluated. The k_{syn}/k_{iso} ratio is reproduced qualitatively with all the methodologies with implicit and explicit solvent.

Scheme 6. Representation of Solvent Attack to the Syndiotactic and Isotactic Propagating Chains

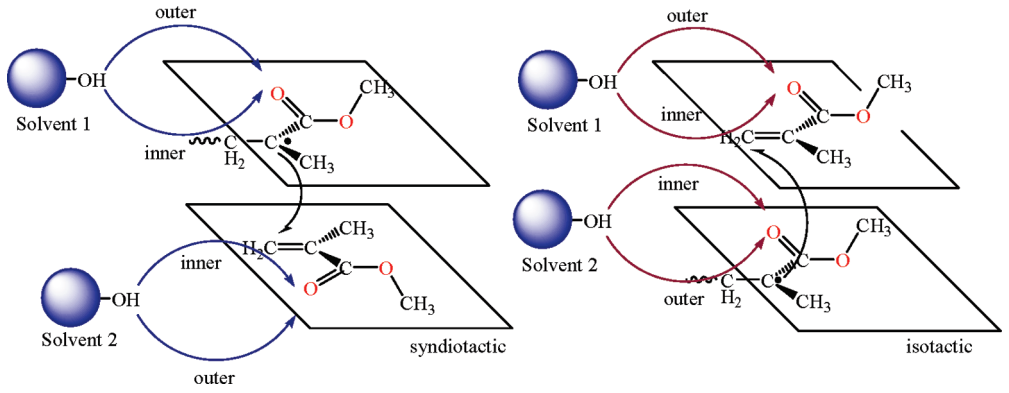

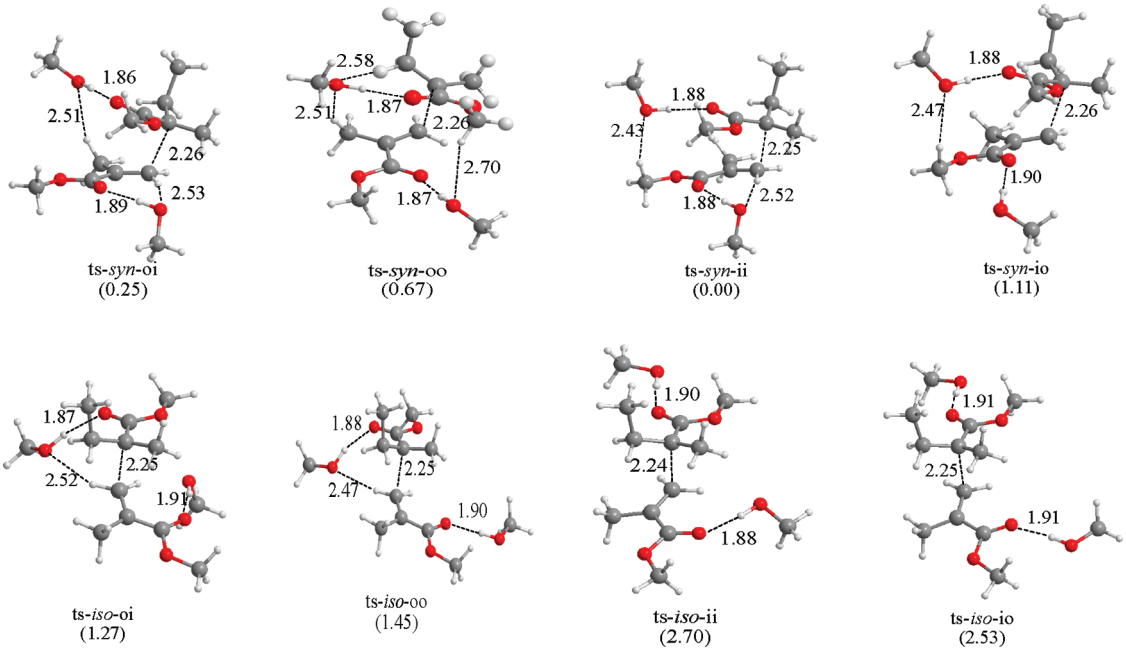

Figure 4. Relative energies (kcal/mol) of the most stable transition structures with CH_3OH (MPWB1K/6-311+G(3df,2p)//B3LYP/6-31+G(d)).

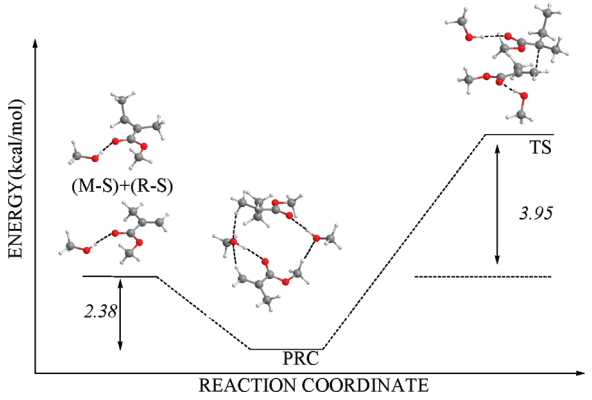

Figure 5. Energetics for syndiotactic dimeric-MMA formation (*syn*-ii) with CH_3OH (MPWB1K/6-311+G(3df,2p)//B3LYP/6-31+G(d)).

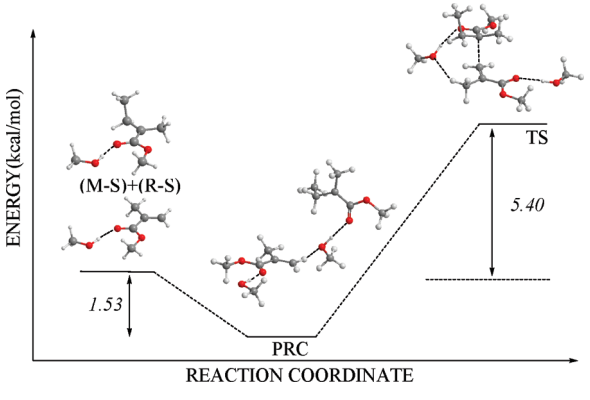

Figure 6. Energetics for isotactic dimeric-MMA formation (*iso*-oo) with CH_3OH (MPWB1K/6-311+G(3df,2p)//B3LYP/6-31+G(d)).

The incorporation of explicit solvent molecules is expected to lead to a decrease in activation energy, resulting in an increase of the reaction rate coefficient as found in a recent work of part of the authors on the effect of explicit water molecules on the propagation rate in acrylamide and methacrylamide.[32] Here the major increase in k_p values results from usage of the explicit/implicit solvation model. As mentioned earlier by Warshell et al., care needs to be taken in absolute evaluation of these values, as this model can also overshoot the solvent effects.[44]

In this study, the presence of explicit and implicit solvent has reproduced qualitatively the experimental expectation in favor of the syndiotactic PMMA.

B. Free Radical Polymerization of MMA in Perfluoro-*tert*-butyl Alcohol $(CF_3)_3COH$. We now investigate the influence of the solvent type on the stereochemistry in MMA polymerization. We have chosen $(CF_3)_3COH$ as the *rr*-tacticity is the largest in this solvent. Four solvated complexes for the monomer MMA−$(CF_3)_3COH$ and radical MMAR−$(CF_3)_3COH$ are found and displayed in Figure 7. They all show a hydrogen bond between the alcoholic H and the carbonyl oxygen, but due to the larger polarizability of $(CF_3)_3COH$ the coordination distance is found slightly smaller (1.75 Å) than the one for methanol (1.90 Å).

In the transition structures along the formation of the syndiotactic and isotactic products notice that the F atoms of the $(CF_3)_3COH$ solvent are in close proximity in the isotactic chains rather than in the syndiotactic chains. The steric repulsion between the bulky solvent molecules is much more pronounced in $(CF_3)_3COH$ rather than in CH_3OH.

In PFTB the reaction barrier for the syndiotactic path (*syn*-ii) is smaller than the one for the isotactic path (*iso*-oi) by about 2.57 kcal/mol due to the presence of steric effects in the isotactic transition structure (Table 4). As displayed in Table 5, the k_{syn}/k_{iso} ratio illustrates the same behavior as the activation barriers in contrast to the FRP of MMA in CH_3OH. The FRP of MMA in PFTB favors the syndiotactic path both energetically and entropically; this is probably due to the nature of the H-bonds which are shorter and stronger in PFTB and stabilize better the pendant groups which are more ordered as compared to the ones in CH_3OH. Also note that the free radical polymerization of MMA in PFTB is exothermic ($\Delta H < 0$) in favor of the syndiotactic path.

The dielectric constant of perfluoro-*tert*-butyl alcohol $(CF_3)_3COH$ has been calculated in order to treat it as a polarizable continuum. The Debye equation has been used to evaluate the dielectric constant of $(CF_3)_3COH$ as shown in eq 6

$$\frac{\varepsilon_r - 1}{\varepsilon_r + 2} = \frac{\rho P_m}{M} \tag{6}$$

ρ is the density of $(CF_3)_3COH$, M is its molecular weight, and P_m is the molar polarization. The formalism displayed in eq 6 has been used to find $\varepsilon = 4.49$ for $(CF_3)_3COH$, and calculations in a continuum with $\varepsilon = 4.49$ have been carried out (Table 5). The experimentally observed enhancement of the stereoselectivity in $(CF_3)_3COH$ is pretty well reproduced qualitatively both with the MPWB1K/6-311+G(3df,2p)//B3LYP/6-31+G(d) and the B2PLYP/6-31+G(d)//B3LYP/6-31+G(d) methodologies.

C. Comparison of the Free Radical Polymerization of MMA in CH_3OH and in $(CF_3)_3COH$. The comparison of activation barriers for the propagation reaction in vacuum, in methanol, and in fluorinated alcohol emphasizes the fact that the solvent stabilizes transition states more than the reactants (Table 6). The reaction barriers $\Delta E_0^{\ddagger}$ for the most favorable reaction paths leading to syndiotactic and isotactic dimeric growing polymer chains are in agreement with the experimental findings at 20 °C where PMMA is 66% syndiotactic in methanol and 75.3% in PFTB, whereas it is 1.2% isotactic in PFTB and 2.5% in methanol respectively (Table 6).[13c] On the energetic and kinetic basis the syndiotactic propagation is accelerated as the interaction with the surrounding medium

Table 2. Energetics (kcal/mol) for Syndiotactic and Isotactic Paths with Explicit CH_3OH at 293.15 K ((MPWB1K/6-311+G(3df,2p)//B3LYP/6-31+G(d))

	$\Delta E_0^{\ddagger}$	$\Delta G^{\ddagger}$	ΔH
syn-oi	4.20	19.73	−17.00
syn-oo	4.62	19.57	−16.50
syn-ii	3.95	19.24	−17.07
syn-io	5.06	19.98	−17.29
iso-oi	5.22	19.40	−16.85
iso-oo	5.40	18.73	−16.94
iso-ii	6.66	19.88	−15.14
iso-io	6.48	19.69	−15.35

Table 3. Kinetics (k_{app}) for the Syndiotactic and Isotactic Polymerization of MMA in Vacuum and CH_3OH at 293.15 K (B3LYP/6-31+G(d) Geometries Have Been Considered)

	B3LYP/6-31 +G(d)	B3LYP/6-311 +G(3df,2p)	MPWB1K/ 6-311+G(3df,2p)	B2PLYP/ 6-31+G(d)
		Explicit Solvent		
$k_{syn\text{-oi}}$	4.82×10^{-7}	6.87×10^{-8}	2.91×10^{-4}	3.71×10^{-3}
$k_{syn\text{-oo}}$	1.68×10^{-6}	2.36×10^{-7}	3.86×10^{-4}	5.87×10^{-3}
$k_{syn\text{-ii}}$	2.09×10^{-6}	2.12×10^{-7}	6.76×10^{-4}	2.06×10^{-2}
$k_{syn\text{-io}}$	1.29×10^{-6}	1.56×10^{-7}	1.89×10^{-4}	4.96×10^{-3}
$k_{iso\text{-oi}}$	2.51×10^{-6}	3.65×10^{-7}	5.12×10^{-4}	5.88×10^{-3}
$k_{iso\text{-oo}}$	6.71×10^{-6}	1.18×10^{-6}	1.64×10^{-3}	3.97×10^{-3}
$k_{iso\text{-ii}}$	1.54×10^{-6}	2.89×10^{-7}	2.26×10^{-4}	7.53×10^{-4}
$k_{iso\text{-io}}$	2.08×10^{-6}	4.08×10^{-7}	3.12×10^{-4}	5.11×10^{-4}
$k_{syn(tot)}$	5.54×10^{-6}	6.73×10^{-7}	1.54×10^{-3}	3.51×10^{-2}
$k_{iso(tot)}$	1.28×10^{-5}	2.24×10^{-6}	2.69×10^{-3}	1.11×10^{-2}
k_{syn}/k_{iso}[a]	0.43	0.30	0.57	3.16
		Implicit + Explicit Solvent		
k_{syn}/k_{iso}[a,b] vacuum		3.85	9.38	40.57
k_{syn}/k_{iso}	0.74	0.68	1.75	
		Implicit Solvent		
k_{syn}/k_{iso}[a,c]		1.04	2.90	

[a] $[k_{syn}/k_{iso}]_{exp} = 22$ in methanol ($[k_{syn}/k_{iso}]_{exp} = 22$ in bulk).[13c] [b] Reaction path within a mixed implicit/explicit solvent model (a solvated monomer and solvated radical embedded in a continuum of dielectric constant $\varepsilon = 32.63$). [c] Reaction path within implicit solvent model embedded in a continuum of dielectric constant $\varepsilon = 32.63$.

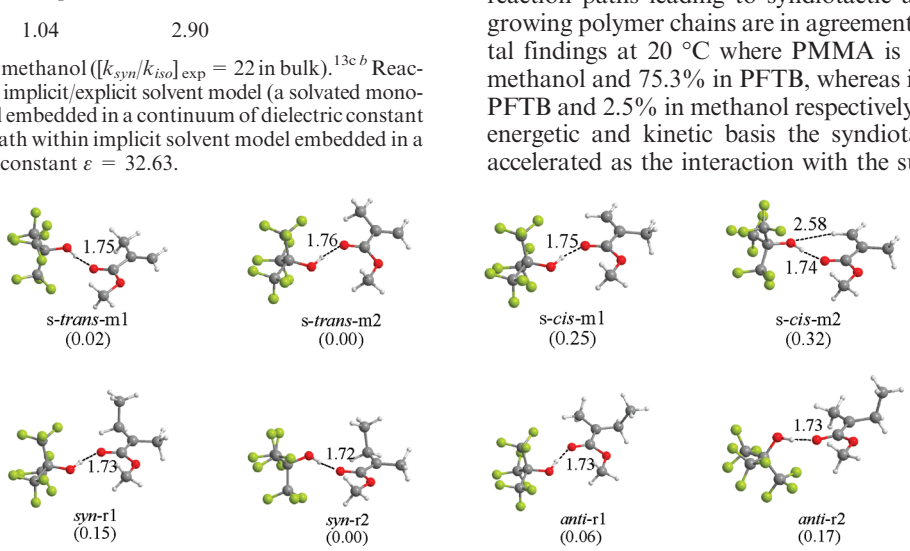

Figure 7. Relative energies (kcal/mol) of MMA−$(CF_3)_3COH$ and MMAR−$(CF_3)_3COH$ complexes (MPWB1K/6-311+G(3df,2p)//B3LYP/6-31+G(d)).

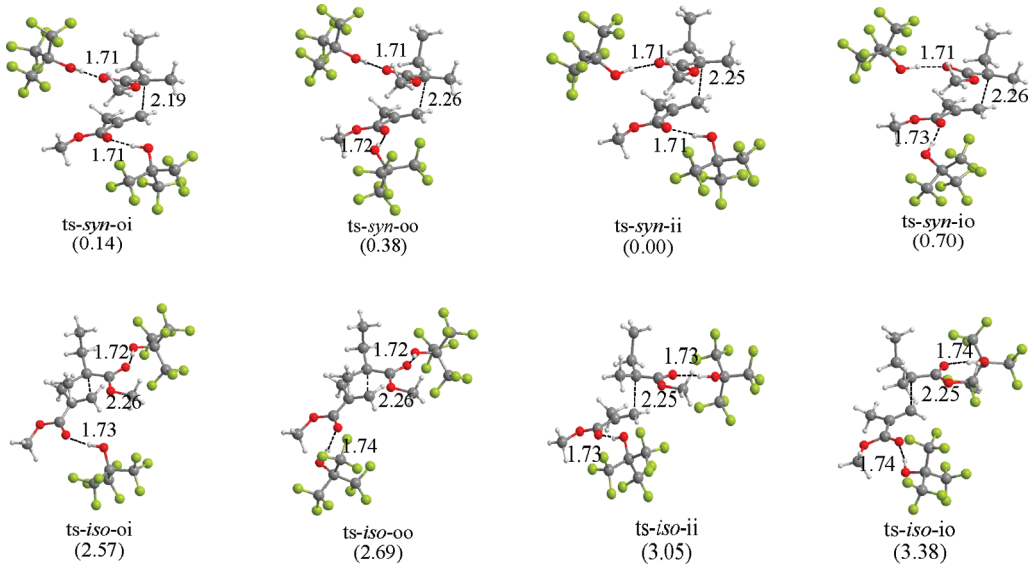

Figure 8. Relative energies (kcal/mol) of the most stable transition structures with $(CF_3)_3COH$ (MPWB1K/6-311+G(3df,2p)//B3LYP/6-31+G(d)).

Table 4. Energetics for Syndiotactic and Isotactic Paths with Explicit $(CF_3)_3COH$ (MPWB1K/6-311+G(3df,2p)//B3LYP/6-31+G(d)) at 293.15 K

	$\Delta E_0^{\ddagger}$	$\Delta G^{\ddagger}$	ΔH
syn-oi	2.97	17.44	−20.23
syn-oo	3.22	18.31	−20.12
syn-ii	2.84	17.10	−19.58
syn-io	3.54	18.47	−19.77
iso-oi	5.41	20.93	−18.06
iso-oo	5.52	20.51	−17.57
iso-ii	5.89	19.86	−16.94
iso-io	6.21	19.10	−16.52

Table 5. Kinetics (k_{app}) for Syndiotactic and Isotactic Polymerization of MMA in Vacuum and $(CF_3)_3COH$ at 293.15 K (B3LYP/6-31+G(d) Geometries Have Been Considered)

	B3LYP/6-31 +G(d)	B3LYP/6-311 +G(3df,2p)	MPWB1K/ 6-311+G(3df,2p)	B2PLYP/ 6-31+G(d)
		Explicit Solvent		
$k_{syn\text{-oi}}$	7.82×10^{-7}	2.13×10^{-6}	1.47×10^{-2}	1.82×10^{0}
$k_{syn\text{-oo}}$	1.80×10^{-7}	4.83×10^{-7}	3.29×10^{-3}	2.55×10^{-1}
$k_{syn\text{-ii}}$	1.38×10^{-6}	3.49×10^{-6}	2.65×10^{-2}	3.25×10^{0}
$k_{syn\text{-io}}$	2.03×10^{-7}	5.21×10^{-7}	2.53×10^{-3}	2.80×10^{-1}
$k_{iso\text{-oi}}$	8.74×10^{-9}	3.14×10^{-8}	3.68×10^{-5}	1.08×10^{-3}
$k_{iso\text{-oo}}$	2.14×10^{-8}	6.38×10^{-8}	7.65×10^{-5}	8.75×10^{-4}
$k_{iso\text{-ii}}$	5.45×10^{-8}	1.73×10^{-7}	2.31×10^{-4}	3.32×10^{-3}
$k_{iso\text{-io}}$	3.09×10^{-7}	9.38×10^{-7}	8.58×10^{-4}	6.26×10^{-3}
$k_{syn(tot)}$	2.55×10^{-6}	6.63×10^{-6}	4.70×10^{-2}	5.61×10^{0}
$k_{iso(tot)}$	3.94×10^{-7}	1.21×10^{-6}	1.20×10^{-3}	1.15×10^{-2}
k_{syn}/k_{iso} [a]	6.47	5.50	39.07	486.06
		Implicit + Explicit Solvent		
k_{syn}/k_{iso} [a,b]		13.19	79.79	477.03
		Vacuum		
k_{syn}/k_{iso} [a]	0.74	0.68	1.75	
		Implicit Solvent		
k_{syn}/k_{iso} [a,c]		1.06	2.85	

[a] $[k_{syn}/k_{iso}]_{exp} = 75$ in $(CF_3)_3COH$.[13c] [b] Reaction path within a mixed implicit/explict solvent model (a solvated monomer and solvated radical embedded in a continuum of dielectric constant $\varepsilon = 4.49$. [c] Reaction path within implicit solvent model embedded in a continuum of dielectric constant $\varepsilon = 4.49$.

Table 6. Reaction Barriers $\Delta E_0^{\ddagger}$ (kcal/mol) and Rate Constants for the Most Favorable Reactions (MPWB1K/6-311+G(3df,2p)//B3LYP/6-31+G(d))

	vacuum	CH_3OH	$(CF_3)_3COH$
$\Delta E_{0(syn)}^{\ddagger}$	5.33	3.95	2.84
$\Delta E_{0(iso)}^{\ddagger}$	6.12	5.40	6.21
k_{syn} [a]		2.17×10^{9}	4.31×10^{10}
k_{iso} [a]		3.03×10^{8}	2.64×10^{8}

[a] Rate constants have been calculated with IEF-PCM in a polar environment.

Table 7. Gas Phase Activation Barriers ($\Delta E_0^{\ddagger}$), Interaction Energies ($\Delta E_{int}^{\ddagger}$), and Distortion Energies ($\Delta E_{dist}^{\ddagger}$) with Explicit Solvent (MPWB1K/6-311+G(3df,2p)//B3LYP/6-31+G(d), kcal/mol)

	CH_3OH			$(CF_3)_3COH$		
	$\Delta E_0^{\ddagger}$	$\Delta E_{int}^{\ddagger}$	$\Delta E_{dist}^{\ddagger}$	$\Delta E_0^{\ddagger}$	$\Delta E_{int}^{\ddagger}$	$\Delta E_{dist}^{\ddagger}$
syn-oi	4.20	−6.64	10.84	2.97	−6.75	9.72
syn-oo	4.62	−6.33	10.95	5.52	−6.59	9.81
syn-ii	3.95	−7.09	11.04	2.84	−6.84	9.67
syn-io	5.06	−5.74	10.79	3.54	−6.33	9.87
iso-oi	5.22	−6.66	11.88	5.41	−4.83	10.24
iso-oo	5.40	−5.71	11.11	5.52	−4.69	10.21
iso-ii	6.66	−4.40	11.05	5.89	−4.61	10.50
iso-io	6.48	−3.27	9.75	6.21	−3.81	10.02

increases. Notice also that the solvent stabilizes less the isotactic transition structures as compared to the syndiotactic ones: for isotactic PMMA even though interactions with the solvent molecules are favorable, their close proximity inhibits this rearrangement. The size of PFTB molecules being larger than the one of CH_3OH molecules there is greater repulsion between PFTB molecules; this behavior is perfectly well reflected in k_{iso} in methanol (3.03×10^8) being larger than k_{iso} in PFTB (2.64×10^8).

The experimentally observed reaction outcomes have also been rationalized by a comparative analysis of the transition state structures via the distortion/interaction model.[45] The activation strain model of chemical reactivity by Bickelhaupt[45b] was employed.

$$\Delta E_0^{\ddagger} = \Delta E_{int}^{\ddagger} + \Delta E_{dist}^{\ddagger} \quad (7)$$

The distortion/interaction model separates the activation energy ($\Delta E_0^{\ddagger}$) into distortion energy ($\Delta E^{\ddagger}_{dist}$) and interaction

energy ($\Delta E^{\ddagger}_{int}$) between distorted fragments, where the former is associated with the strain caused by deforming the individual reactants and the latter is the favorable interaction between the deformed reactants.

When CH_3OH is the solvent, the contribution of the distortion energy is more or less similar for both sydiotactic and isotactic channels. On the other hand, when $(CF_3)_3COH$ is used, the distortion energy is higher in the isotactic channel as expected based on the proximity of the pendant groups. Also in $(CF_3)_3COH$, the interaction energies stabilize the syndiotactic structures more than the isotactic ones; this is confirmed by the stronger H-bonds (1.71 Å) in these structures as compared to the ones in the syndiotactic structures (1.72−1.74 Å). Overall, the distortion/interaction model explains the experimentally determined syndiotactic preference of the free radical polymerization of MMA in the presence of $(CF_3)_3COH$.

Conclusion

In this study, the control of the stereochemistry in methyl methacrylate (MMA) has been modeled with the B3LYP/6-31+G(d)//B3LYP/6-31+G(d), B3LYP/6-311+G(3df,2p)//B3LYP/6-31+G(d), MPWB1K/6-311+G(3df,2p)//B3LYP/6-31+G(d), and B2PLYP/6-31+G(d)//B3LYP/6-31+G(d) methodologies. The role of the solvent on the tacticity of MMA polymerization has been investigated by considering the propagation rate constants for the syndiotactic and isotactic free radical polymerization of MMA in vacuum, in methanol (CH_3OH), and in 1,1,1,3,3,3-hexafluoro-2-(trifluoromethyl)propan-2-ol ($(CF_3)_3COH$). The role of $(CF_3)_3COH$ in inhibiting the isotacticity of PMMA has been explained by the steric hindrance of the pendant solvent molecules strongly hydrogen bonded to the carbonyl oxygens (∼1.7 Å) located on the same side of the backbone. CH_3OH is less effective in reducing the isotacticity because of its small size and because of the relatively loose hydrogen bonds (∼1.9 Å) with the carbonyl oxygen. The methodologies used in this study within the scope of the terminal unit model have effectively reproduced the solvent effect on the FRP kinetics of MMA. The quantitative reproduction of absolute rates of polymerization in solvent remains a challenge for theoretical methods; however, this study proves that qualitative trends on effect of solvent on tacticity can be reproduced by the used theoretical models. Overall, this study has demonstrated the fact that computational chemistry offers a viable alternative to experiment: the effect of solvent on tacticity can be predicted prior to the experiment.

Acknowledgment. The computational resources used in this work were provided by the TUBITAK ULAKBIM High Performance Computing Center, the Bogazici University Research Foundation (Project 08M101), and the National Center for High Performance Computing of Turkey (UYBHM) under Grant 20502009. The authors acknowledge for funding the travel and lodging expenses of I.D., V.A., and V.V.S. in UG and BU and the sixth framework project COSBIOM (FP6-2004-ACC-SSA-2.517991). The UGent authors thank the FWO (Fonds voor Wetenschappelijk Onderzoek - Vlaanderen, Fund for Scientific Research - Flanders), the research board of Ghent University for the bilateral project Ghent - Istanbul, and the IAP-BELSPO project in the frame of IAP 6/27 for financial support of this research. Part of this work has also made use of the computational resources and services provided by Ghent University.

Supporting Information Available: Tables of optimized geometries, total energies, enthalpies, Gibbs free energies, and solvation energies for all structures discussed in this study. This material is available free of charge via the Internet at http://pubs.acs.org.

References and Notes

(1) Gladysz, J. A. *Chem. Rev.* **2000**, *100*, 1167–1168.
(2) Sugiyama, Y.; Satoh, K.; Kamigaito, M.; Okamoto, Y. *J. Polym. Sci., Part A: Polym. Chem.* **2006**, *44*, 2086–2098.
(3) (a) Pino, P.; Suter, U. W. *Polymer* **1976**, *17*, 977–995. (b) Hatada, K.; Kitayama, T.; Ute, K. *Prog. Polym. Sci.* **1988**, *13*, 189–276. (c) Yuki, H.; Hatada, K. *Adv. Polym. Sci.* **1979**, *31*, 1–45.
(4) Matsumoto, A. In *Handbook of Radical Polymerization*; Matyjaszewski, K., Davis, T. P., Eds.; Wiley-Interscience: Hoboken, NJ, 2002; pp 691−773.
(5) (a) Habaue, S.; Okamoto, Y. *Chem. Rec.* **2001**, *1*, 46–52. (b) Miura, Y.; Shibata, T.; Satoh, K.; Kamigaito, M.; Okamoto, Y. *J. Am. Chem. Soc.* **2006**, *128*, 16026–16027.
(6) Tanaka, H. *Prog. Polym. Sci.* **1992**, *17*, 1107–1152.
(7) Satoh, K.; Kamigaito, M. *Chem. Rev.* **2009**, *109*, 5120–5156.
(8) Isobe, Y.; Nakano, T.; Okamoto, Y. *J. Polym. Sci., Part A: Polym. Chem.* **2001**, *39*, 1463–1471.
(9) Isobe, Y.; Fujioka, D.; Habaue, S.; Okamoto, Y. *J. Am. Chem. Soc.* **2001**, *123*, 7180–7181.
(10) Habaue, S.; Isobe, Y.; Okamoto, Y. *Tetrahedron* **2002**, *58*, 8205–8209.
(11) Okamoto, Y.; Habaue, S.; Isobe, Y.; Suito, Y. *Macromol. Symp.* **2003**, *195*, 75–80.
(12) Suito, Y.; Isobe, Y.; Habaue, S.; Okamoto, Y. *J. Polym. Sci., Part A: Polym. Chem.* **2002**, *40*, 2496–2500.
(13) (a) Yamada, K.; Nakano, T.; Okamoto, Y. *Macromolecules* **1998**, *31*, 7598–7605. (b) Isobe, Y.; Yamada, K.; Nakano, T.; Okamoto, Y. *Macromolecules* **1999**, *32*, 5979–5981. (c) Isobe, Y.; Yamada, K.; Nakano, T.; Okamoto, Y. *J. Polym. Sci., Part A: Polym. Chem.* **2000**, *38*, 4693–4703.
(14) Miura, Y.; Satoh, T.; Narumi, A.; Nishizawa, O.; Okamoto, Y.; Kakuchi, T. *J. Polym. Sci., Part A: Polym. Chem.* **2006**, *44*, 1436–1446.
(15) (a) Miura, Y.; Satoh, T.; Narumi, A.; Nishizawa, O.; Okamoto, Y.; Kakuchi, T. *Macromolecules* **2005**, *38*, 1041–1043. (b) Miura, Y.; Satoh, T.; Narumi, A.; Nishizawa, O.; Okamoto, Y.; Kakuchi, T. *J. Polym. Sci., Part A: Polym. Chem.* **2006**, *44*, 1436–1446.
(16) Tanaka, H.; Niwa, M. *Polymer* **2008**, *49*, 3693–3701.
(17) Nakano, T.; Okamoto, Y. In *Controlled Radical Polymerization*; Matyjazsewski, K., Ed.; ACS Symposium Series 685; American Chemical Society: Washington, DC, 1998; pp 451−462.
(18) Beuermann, S. *Macromol. Rapid Commun.* **2009**, *30*, 1066–1088.
(19) O'Driscoli, K. F.; Monteiro, M. J.; Klumperman, B. *J. Polym. Sci., Part A: Polym. Chem.* **1997**, *35*, 515–520.
(20) Zammit, M. D.; Davis, T. P.; Willett, G. D.; O'Driscoli, K. F. *J. Polym. Sci., Part A: Polym. Chem.* **1997**, *35*, 2311–2321.
(21) Harrisson, S.; Barner-Kowollik, C.; Davis, T. P.; Evans, K.; Rizzardo, R.; Stenzel, M.; Yin, M. *Z. Phys. Chem.* **2005**, *219*, 267–281.
(22) Ganachaud, F.; Balic, R.; Monteiro, M. J.; Gilbert, R. G. *Macromolecules* **2000**, *33*, 8589–8596. Seabrook, S. A.; Tonge, M. P.; Gilbert, R. G. *J. Polym. Sci., Part A: Polym. Chem.* **2005**, *43*, 1357–1368.
(23) Frisch, M. J.; Trucks, G. W.; Schlegel, H. B.; Scuseria, G. E.; Robb, M. A.; Cheeseman, J. R.; Montgomery, Jr., J. A.; Vreven, T.; Kudin, K. N.; Burant, J. C.; Millam, J. M.; Iyengar, S. S.; Tomasi, J.; Barone, V.; Mennucci, B.; Cossi, M.; Scalmani, G.; Rega, N.; Petersson, G. A.; Nakatsuji, H.; Hada, M.; Ehara, M.; Toyota, K.; Fukuda, R.; Hasegawa, J.; Ishida, M.; Nakajima, T.; Honda, Y.; Kitao, O.; Nakai, H.; Klene, M.; Li, X.; Knox, J. E.; Hratchian, H. P.; Cross, J. B.; Bakken, V.; Adamo, C.; Jaramillo, J.; Gomperts, R.; Stratmann, R. E.; Yazyev, O.; Austin, A. J.; Cammi, R.; Pomelli, C.; Ochterski, J. W.; Ayala, P. Y.; Morokuma, K.; Voth, G. A.; Salvador, P.; Dannenberg, J. J.; Zakrzewski, V. G.; Dapprich, S.; Daniels, A. D.; Strain, M. C.; Farkas, O.; Malick, D. K.; Rabuck, A. D.; Raghavachari, K.; Foresman, J. B.; Ortiz, J. V.; Cui, Q.; Baboul, A. G.; Clifford, S.; Cioslowski, J.; Stefanov, B. B.; Liu, G.; Liashenko, A.; Piskorz, P.; Komaromi, I.; Martin, R. L.; Fox, D. J.; Keith, T.; Al-Laham, M. A.; Peng, C. Y.; Nanayakkara, A.; Challacombe, M.; Gill, P. M. W.; Johnson, B.; Chen, W.; Wong, M. W.; Gonzalez, C.; Pople, J. A. *Gaussian 03, Revision D.01*; Gaussian Inc.: Wallingford, CT, 2004.
(24) Smith, D. M.; Nicolaides, A.; Golding, B. T.; Radom, L. *J. Am. Chem. Soc.* **1998**, *120*, 10223–10233.
(25) Gonzáles, C.; Schlegel, H. B. *J. Phys. Chem.* **1990**, *94*, 5523–5527.
(26) Zhao, Y.; Truhlar, D. G. *J. Phys. Chem. A* **2004**, *108*, 6908–6918.
(27) Furuncuoğlu, T.; Uğur, İ.; Değirmenci, İ.; Aviyente, V. *Macromolecules* **2010**, *43*, 1823–1835.

(28) Liang, K.; Dossi, M.; Moscatelli, D.; Hutchinson, R. A. *Macromolecules* **2009**, *42*, 7736–7744.
(29) Yu, X.; Pfaendtner, J.; Broadbelt, L. J. *J. Phys. Chem. A* **2008**, *112*, 6772–6782.
(30) (a) Lee, C. T.; Yang, W. T.; Parr, R. G. *Phys. Rev. B* **1988**, *37*, 785–789. (b) Becke, A. D. *Phys. Rev. A* **1988**, *38*, 3098–3100.
(31) (a) Grimme, S.; Steinmetz, M.; Korth, M. *J. Chem. Theory Comput.* **2007**, *3*, 42–45. (b) Grimme, S. *J. Chem. Phys.* **2006**, *124*, 174301–12.
(32) De Sterck, B.; Roel Vaneerdeweg, R.; Du Prez, F.; Waroquier, M; Van Speybroeck, V. *Macromolecules* **2010**, *43*, 827–836.
(33) Singleton, D. L.; Cvetanovic, R. J. *J. Am. Chem. Soc.* **1976**, *98*, 6812–6819.
(34) Pilling, M. J.; Seakins, P. W. *Reaction Kinetics*; Oxford University Press: New York, 1996.
(35) *Atkins' Physical Chemistry*, 8th ed.; Atkins, P., De Paula, J., Eds.; Oxford University Press: New York, 2006.
(36) (a) Tomasi, J.; Mennucci, B.; Cancès, E. *J. Mol. Struct.: THEOCHEM* **1999**, *464*, 211–226. (b) Cancès, M. T.; Mennucci, B.; Tomasi, J. *J. Chem. Phys.* **1997**, *107*, 3032–3041. (c) Mennucci, B.; Tomasi, J. *J. Chem. Phys.* **1997**, *106*, 5151–5158. (d) Mennucci, B.; Cancès, E.; Tomasi, J. *J. Phys. Chem. B* **1997**, *101*, 10506–10517.
(37) (a) Kelly, C. P.; Cramer, C. J.; Truhlar, D. G. *J. Phys. Chem. A* **2006**, *110*, 2493–2499. (b) Kamerlin, S. C. L.; Haranczyk, M.; Warshel, A. *ChemPhysChem* **2009**, *10*, 1125–1134. (c) De Sterck, B.; Van Speybroeck, V.; Mangelinckx, S.; Verniest, G.; De Kimpe, N.; Waroquier, M. *J. Phys. Chem. A* **2009**, *113*, 6375–6380. (d) Van Speybroeck, V.; Moonen, K.; Hemelsoet, K.; Stevens, C.; Waroquier, M. *J. Am. Chem. Soc.* **2006**, *128*, 8468–8478. (e) Kelly, C. P.; Cramer, C. J.; Truhlar, D. G. *J. Chem. Theory Comput.* **2005**, *1*, 1133–1152.
(38) (a) Heuts, J. P. A.; Gilbert, R. G.; Radom, L. *Macromolecules* **1995**, *28*, 8771–8781. (b) Wong, M. W.; Radom, L. *J. Phys. Chem.* **1995**, *99*, 8582–8588. (c) Heuts, J. P. A.; Gilbert, R. G.; Radom, L. *J. Phys. Chem.* **1996**, *100*, 18997–19006. (d) Wong, M. W.; Radom, L. *J. Phys. Chem. A* **1998**, *102*, 2237–2245. (e) Fischer, H.; Radom, L. *Angew. Chem., Int. Ed.* **2001**, *40*, 1340–1371. (f) Gómez-Balderas, R.; Coote, M. L.; Henry, D. J.; Fischer, H.; Radom, L. *J. Phys. Chem. A* **2003**, *107*, 6082–6090. (g) Gómez-Balderas, R.; Coote, M. L.; Henry, D. J.; Radom, L. *J. Phys. Chem. A* **2004**, *108*, 2874–2883. (h) Henry, D. J.; Coote, M. L.; Gómez-Balderas, R.; Radom, L. *J. Am. Chem. Soc.* **2004**, *126*, 1732–1740.
(39) Izgorodina, E. I.; Coote, M. L. *Chem. Phys.* **2006**, *324*, 96–110.
(40) Coote, M. L. *Macromol. Theory Simul.* **2009**, *18*, 388–400.
(41) Lin, C. Y.; Izgorodina, E. I.; Coote, M. L. *Macromolecules* **2010**, *43*, 553–560.
(42) Van Cauter, K.; Van Speybroeck, V.; Waroquier, M. *ChemPhysChem* **2007**, *8*, 541–552.
(43) (a) Değirmenci, İ.; Aviyente, V.; Van Speybroeck, V.; Waroquier, M. *Macromolecules* **2009**, *42*, 3033–3041. (b) Değirmenci, İ.; Avcı, D.; Aviyente, V.; Van Cauter, K.; Van Speybroeck, V.; Waroquier, M. *Macromolecules* **2007**, *40*, 9590–9602. (c) Günaydın, H.; Seyhan, S.; Tüzün, N. Ş.; Avcı, D.; Aviyente, V. *Int. J. Quantum Chem.* **2005**, *103*, 176–189. (d) Salman, S.; Ziylan Albayrak, A.; Avcı, D.; Aviyente, V. *J. Polym. Sci., Part A: Polym. Chem.* **2005**, *43*, 2574–2583.
(44) Kamerlin, S. C. L.; Haranczyk, M.; Warshel, A. *ChemPhysChem* **2009**, *10*, 1125–1134.
(45) (a) Ess, D. H.; Houk, K. N. *J. Am. Chem. Soc.* **2007**, *129*, 10646. (b) Bento, A. P.; Bickelhaupt, F. M. *J. Org. Chem.* **2008**, *73*, 7290–7299. (c) Catak, S.; Matthias D'hooghe, M.; De Kimpe, N.; Waroquier, M.; Van Speybroeck, V. *J. Org. Chem.* **2010**, *75*, 885–896.